# Evaluation and Optimization of Dozing Operations for Small-Scale Wheeled Vehicles with Simulation and Validation Using a Reference Platform

Gregory Ryan Colvin

CMU-RI-TR-16-13

*Submitted in partial fulfillment of the*
*Requirements for the degree of*
*Masters of Science in Robotics*

The Robotics Institute
Carnegie Mellon University
Pittsburgh, Pennsylvania 15213

April 2016

Masters Committee:
Dimitrios Apostolopoulos, Chair
David Wettergreen
Nathan Otten

## Abstract

Currently the majority of dozing operations are conducted using tracked vehicles with a fixed blade cutting angle. There is interest from industry in exploring alternatives to tracked vehicles for small scale dozing operations because of the limitations of the platform. One alternative is a six-wheeled vehicle with independent drives and an active suspension. This alternative has higher mobility and controllability than tracked vehicles, but generally produces less traction. This decrease in traction leads to lower dozing ability when compared to tracked vehicles. The purpose of this thesis is to study the process of robotic dozing and understand the value and limitations of dozing with wheeled vehicles. This study focuses on the evaluation and design of the blade and vehicle suspension as major contributors in dozing operations.

To begin, the blade-soil fundamentals were studied and it was found that there could be large increase in dozing performance if the blade was changed from a traditional vertical angle to a variable attack angle. Therefore, a variable angle blade design that would decrease the power required for dozing application was investigated. The forces experienced during dozing were derived and an optimization was developed to change the blade angle in response to different dozing conditions. This new design and control is shown to increase the dozing ability when compared to a vertical blade. For shallow dozing, this a variable angle blade can reduce the overall push force required up to 75% while reducing the total volume per swipe by only 15%.

Following the evaluation of a new blade design the second component, the suspension, was investigated. First, a simplified version of the reference robot being studied was constructed in CAD and imported into SimMechanics. Next, in a joint MatLab SimMechanics interface, a simulation of varying suspension properties and the robot operating environment was created. The simulation was then validated with physical testing of the robot. Following validation, an optimization program was written such that the optimal suspension properties are determined for different operation scenarios. The use of this semi-active suspension has shown to increase the applied force for the wheels up to 16 percent. To conclude the study, three case studies which combine the new blade design and the SimMechanics suspension optimization are presented.

## Acknowledgements

I would like to thank my advisor Professor Dimi Apostolopoulos for his support and guidance throughout this project. In addition, I would like to thank my thesis committee members Prof. David Wettergreen and Ph.D. candidate Nate Otten for their help and feedback. Finally, I would also like to acknowledge Rich Pantaleo and the rest of the NREC staff for their support of this project and other academic projects.

# Contents

1 Introduction ..... 1
1.1 Motivation ..... 1
1.2 Objective & Approach ..... 2
1.3 Thesis Overview ..... 2
2 Blade Design & Optimization ..... 3
2.1 Blade Cutting Model ..... 3
2.1.1 Modified McKyes Approach ..... 3
2.1.2 Volumetric Analysis ..... 6
2.2 Simulation & Optimization ..... 7
2.2.1 MatLab Simulation ..... 7
2.2.2 Optimization ..... 9
2.3 Discussion ..... 12
3 Suspension Study ..... 13
3.1 Vehicle Model ..... 14
3.2 Suspension Study ..... 18
3.2.1 Model Verification ..... 18
3.2.2 Suspension Optimization ..... 20
3.3 Discussion ..... 22
4 Combined Model ..... 23
4.1 Blade Design ..... 23
4.2 Updated Model ..... 24
4.3 Example Cases ..... 25
4.3.1 Forward Driving & Dozing ..... 25
4.3.2 Reverse Driving & Dozing ..... 27
4.3.3Suspension Tuning ..... 28
4.4 Discussion ..... 29
5 Conclusion ..... 30
5.1 Summary and conclusions ..... 30
5.2 Contribution ..... 30
5.3 Future Work ..... 31
References ..... 32

## List of Figures

Figure 1: 6x6 Utility Robot Outfitted for Mapping Operations....1
Figure 2: Force Breakdown for McKyes Model....4
Figure 3: Volumetric Analysis....6
Figure 4: Forces for Varying Blade Angles at 15cm....7
Figure 5: Forces for Varying Blade Angles at 35 cm....8
Figure 6: Individual Metrics and Overall Cost Function for Blade Angle Optimization....10
Figure 7: Optimum Angle at 15 cm....11
Figure 8: Optimum Angle at 35 cm....11
Figure 9: Current Draw for 6x6 Robot....13
Figure 10: Robot Being Studied....14
Figure 11: Kinematic Breakdown....15
Figure 12: Robot Components and References....15
Figure 13: SimMechanics Code of Robot....16
Figure 14: Swing Arm and Suspension Code....17
Figure 15: Completed Model....17
Figure 16: Lifted Robot Over Scales with Varied Pre-Loads....18
Figure 17: Robot with Added Weight....19
Figure 18: Search Procedure....21
Figure 19: Variable Angle Blade Design....23
Figure 20: SimMechanics Code for Combined Model....24
Figure 21: Combined Model....24
Figure 22: Reverse Driving and Dozing....27
Figure 23: Suspension Tuning Table....28
Figure 24: Suspension Tuning Results....28

## List of Tables

Table 1: Validation Results.....20
Table 2: Flat Driving & Dozing Comparison .....26
Table 3: Flat Driving & Dozing in Reverse Comparison .....27

# Nomenclature

| | |
|---|---|
| $\alpha$ | Blade Angle [degrees °] |
| $\beta$ | Failure Plane Angle [degrees °] |
| $\delta$ | Soil/Blade Friction Angle [degrees °] |
| $\varphi$ | Soil Internal Friction Angle [degrees °] |
| $\gamma$ | Soil Density [kg/m$^3$] |
| v | Velocity [m/s] |
| W | Weight of Wedge [N] |
| $W_b$ | Weight of Blade [N] |
| Q | Surcharge [N] |
| h | Overall Height of Blade [m] |
| d | Cutting Depth [m] |
| w | Blade Width [m] |
| C | Cohesion [pa] |
| $C_a$ | Adhesion [pa] |
| $L_f$ | Failure Plane Length [m] |
| $L_b$ | Blade Length [m] |
| $V_{max}$ | Max Volume Per Swipe [m$^3$] |
| $L_{max}$ | Max Distance Per Swipe [m] |
| R | Soil Reaction Force [N] |
| q | Force Due to Surcharge [N] |
| F | Force Applied to Blade [N] |
| H | Horizontal Force Applied to Blade [N] |
| V | Vertical Force Applied to Blade [N] |

## 1.1 Introduction

Robotic dozing is being explored by industry because it reduces costs, increases job site safety, and allows for 24 hour operation. [1][2][3] Currently, the majority of dozing operations are conducted using tracked vehicles with a fixed blade. There is interest from industry in exploring alternatives to tracked vehicles for small scale dozing operations because of the limitations of tracked vehicles. Tracked vehicles are suitable for dozing applications because they provide substantial reaction to workloads while maintaining excellent traction. When compared to wheeled vehicles, tracked vehicles generally have less handling and controllability, consume more power, and generally operate at slower speeds. For this reason, the majority of non-dozing robotic vehicles are wheeled. An example of a wheeled robotic utility vehicle is shown below in Figure 1. This vehicle is currently used for mapping and other tasks, but there is interest in expanding the operation of this vehicle to dozing as well. Using this vehicle for dozing would decrease the number of robots required on a job site, increase the handling and controllability during dozing operations, and could take advantage of the automation already completed for the robot.

The purpose of this thesis is to study robotic dozing and evaluate the merit of using wheeled vehicles for light dozing operations. This study was completed using the reference platform shown in Figure 1, but the results can be generalized to other platforms. After evaluation of the robot it was found that the two main contributors to dozing performance were the blade design and the suspension configuration. For this reason, this study focuses on improving overall dozing performance by evaluating and optimizing the blade design and vehicle suspension.

Figure 1: 6x6 Utility Robot Outfitted for Mapping Operations

## 1.1 Motivation

A mining company currently employs two robots in its operations. One is a tracked vehicle which is used for dozing recently blasted areas of the mine. The second is a 6x6 wheeled vehicle, shown in Figure 1, which is used for autonomously mapping the mine. It would be

advantageous if both of these jobs could be completed by one robot. To travel throughout the mine, for mapping and other reasons, there are large steps which the robot has to climb and descend which a tracked vehicle would not be able to complete. In comparison the dozing operations do not require any specific performance which would rule out a wheeled vehicle. In addition, wheeled vehicles have greater mobility, less power consumption, and greater speed range when compared to tracked vehicles. The disadvantage of using a wheeled vehicle instead of a tracked vehicle is the decrease in forward push force.

This thesis is a study of using wheeled vehicles for dozing operations which are currently being conducted by tracked vehicles. There are many benefits to wheeled vehicles, but the decrease in overall push force is a large concern. Techniques to help increase the effectiveness of wheeled vehicles are the main focus of this research.

## 1.2 Objective & Approach

The objective of this research is to characterize the design space, capabilities, and limitations of wheeled robotic dozing. This thesis focuses on the study and design of the blade and suspension as major contributors in wheeled dozing operations. A 6x6 robotic vehicle, shown in Figure 1, is used as a reference platform. Models and simulations for the blade and suspension are built, studied, and optimized. Finally, these components are recombined in a single simulation and evaluated.

## 1.3 Thesis Overview

Chapter 2 presents the first component of this study, which is an investigation of replacing standard vertical blades with an optimized variable angle blade. Chapter 3 covers the second component of this study, the addition of a semi-active suspension to improve upon the overall performance of the vehicle. The next chapter, Chapter 4, recombines the blade and suspension into one simulation and provides example test cases for the use of both a variable angle blade and a semi-active suspension. Finally, Chapter 5 presents a summary and conclusion of the work presented and makes recommendations for the continuation of this research.

# 2 Blade Design & Optimization

Blade cutting and dozing models were explored and it was found that McKyes model is widely used and accepted in the field.[4][5][6][7] This model takes into account the blade geometry, soil properties, and cutting depth to calculate the horizontal and vertical forces on the blade. The model is then modified by adding a term to account for dynamics, as well as adding a volumetric analysis. Once this was completed and verified with published results [4], many different situations were simulated showing how the efficiency of the blade changes under varying conditions. While the simulation allows the user to change all of the variables presented in the following sections, it is most relevant for this study is to see how the dozing forces change for different soils, varying cutting depths, and different speeds of operation.

From these simulations, metrics were developed in order to construct an optimization for the blade cutting angle. The first metric calculates the amount of material moved per power input, the second shows the amount of material moved per time step and the final metric takes into account the total volume moved per swipe. These metrics were normalized individually, weighted, and added together to build a cost function in terms of blade angle and robot speed. Using this cost function, an optimization program is used to find the ideal blade cutting angle.

## 2.1 Blade Cutting Model

### *2.1.1 Modified McKyes Approach*

McKyes [5] approach is built from the general wedge theory of soil mechanics. Soil failure caused by a moving blade can be approximated by soil failure planes, which cause discrete wedges of soil to be moved. This is illustrated in Figure 2.The outlined black shape is the blade which is moving through the soil. The dotted line shows the actual failure planes caused by the blade, while the wedge defined by $\alpha$ and $\beta$ shows the approximated version of the failure planes. The force W is the weight of the soil contained in the failure wedge. Q is the weight of the soil piled above the failure wedge and is called the surcharge. The force $cL_f$ is the force caused by the cohesion of moving the soil over itself, and similarly, the force $c_aL_b$ is the force caused by the adhesion of the soil moving against the blade. R is the reaction force of the uncut soil in response to the force needed to cause the failure planes. A table of all variables can be found in the nomenclature section on page VI. All of the forces on the wedge are summed to find the force F needed to cut and move the soil.

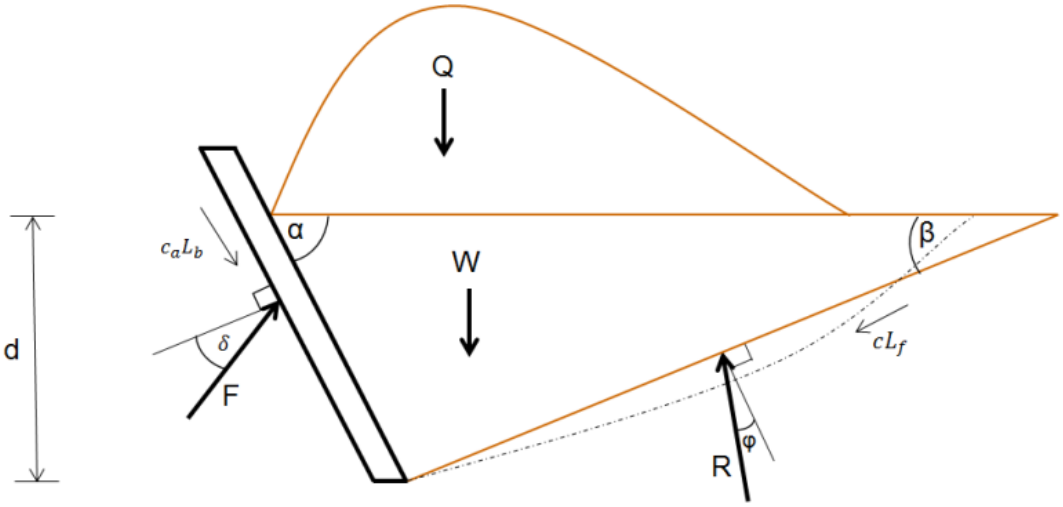


Figure 2: Force Breakdown for McKyes Model

$$F = \frac{[W+Q]\,sin(\beta-\varphi) + cL_f\,cos\,\varphi + c_aL_b[cos(\alpha+\beta)+sin(\alpha+\beta)]\,cos\,\varphi}{sin(\alpha+\beta-\delta-\varphi)}$$

This equation is then rewritten into the 'Universal Earth Moving Equation':

$$F = \left[\gamma d^2K_p + cdK_c + C_adK_{ca} + qdK_q\right]w$$

Where the surcharge is:

$$q = \frac{\gamma gl\,tan\,\beta\,tan\,\alpha}{2(tan\,\beta + tan\,\alpha)}$$

And the K values are passive parameters dependent on φ, $\delta$, α, and β:

$$K_p = \frac{(cot\,\alpha + cot\,\beta)\,sin(\beta+\varphi)}{2\,sin(\alpha+\beta+\delta+\varphi)}$$

$$K_c = \frac{cos\,\varphi}{sin\,\beta\,sin(\alpha+\beta+\delta+\varphi)}$$

$$K_{ca} = \frac{-cos(\alpha+\beta+\varphi)}{sin\,\beta\,sin(\alpha+\beta+\delta+\varphi)}$$

$$K_q = 2K_p$$

All of the parameters are known except β, the failure plane angle. Coulomb proposed that the soil would shear along the path of least resistance. Therefore, the most appropriate angle of failure is one which does not depend on the soil cohesion or adhesion, but causes $K_p$ to be minimum. This yields:

$$\beta = \cot^{-1}\left[\frac{\sqrt{\frac{\sin(\alpha+\delta)\sin(\delta+\varphi)}{\sin\alpha\sin\varphi}} - \cos(\alpha+\delta+\varphi)}{\sin(\alpha+\delta+\varphi)}\right]$$

The model presented above is McKyes approach. Previous research has shown that the addition of a dynamic term can increase the accuracy of the model. [4] After adding a dynamic term to account for speed the Universal Earth moving Equation becomes:

$$F = \left[\gamma d^2 K_p + cdK_c + C_a dK_{ca} + qdK_q + \gamma v^2 dK_a\right]w$$

Where:

$$K_a = \frac{\tan(\beta) + \cot(\beta+\varphi)}{[\cos(\alpha+\beta) + \sin(\alpha+\delta)\cot(\beta+\varphi)][\tan(\beta)\cot(\alpha)]}$$

Now the horizontal component of the dozing force, H, acting on the blade can be found as:

$$H = \mathrm{F}\sin(\alpha+\delta) + C_a\,\mathrm{dw}\cot\alpha$$

Where the first term is the result of the wedge theory and the second term is an added friction term. The vertical component of the dozing force, V, is:

$$V = \mathrm{F}\cos(\alpha+\delta) - C_a dw + W_b$$

Where the first term is the result of the wedge theory, the second term is an added friction term, and $W_b$ is the weight of the blade.

### *2.1.2 Volumetric Analysis*

In order to generate a more complete model of dozing, a model of the amount of material being dozed was created and is shown in Figure 3. $V_1$ is the volume of the pile already moved.

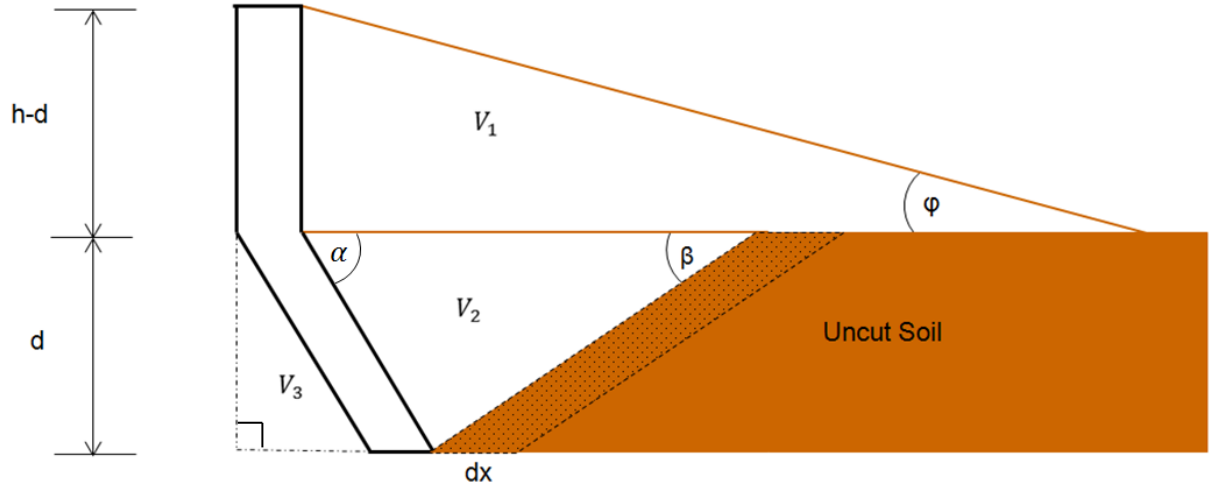


Figure 3: Volumetric Analysis

This volume is approximated by the right triangle defined by the height of the blade above the cutting surface, h-d, the soil internal friction angle φ, and the width of the blade w. The distance d is assumed to be even with the top of the soil in order to simplify the model. Once this volume is reached the soil will begin to overflow onto the robot. This volume is used to determine the maximum volume and distance a certain blade can move per swipe. The equation for $V_1$ is:

$$V_1 = \frac{w(h-d)^2}{2\,tan\,\varphi}$$

The second volume, $V_2$, is the size of the wedge being cut at each point in time and was explained in the previous section. $V_2$ is found as:

$$V_2 = \frac{wd^2}{2}\left[\frac{1}{tan\,\beta} + \frac{1}{tan\,\alpha}\right]$$

The final volume, $V_3$, is the volume to be displaced in order to engage the blade. This is a function of the blade angle α and the cutting depth d, as seen below:

$$V_3 = \frac{wd^2}{2tan\,\alpha}$$

With an angled blade, if the blade is pushed into the soil and then removed it is likely that the displaced soil, or cost to engage, will fall back into the void created in the initial push. In

addition, $V_2$ has been cut, but it has not been displaced, so for this application it will not be factored into the total volume moved. Using these two assumptions the max volume which can be displaced per swipe can be written as the volume of the pile minus the cost to engage. This max volume is shown below:

$$V_{max} = \frac{w(h-d)^2}{2\,tan\,\varphi} - \frac{wd^2}{2tan\,\alpha}$$

## 2.2 Simulation & Optimization

### *2.2.1 MatLab Simulation*

The modified McKyes model and the volumetric analysis were added together and formed into a simulation using MatLab. The first goal of the simulation was to compare the required horizontal force per swipe for varying blade angles, α. Many simulations with various parameters were completed. Simulation results with properties for stewiacke soil taken from Onwualu and Watts [4] are shown below.

$\rightarrow \varphi = 30°$
$\rightarrow \delta = 15°$
$\rightarrow w = 25.4\ cm$
$\rightarrow v = 1\ \frac{m}{s}$
$\rightarrow d = 15\ cm$
$\rightarrow h = 75\ cm$
$\rightarrow C = 2000\ pa$
$\rightarrow C_a = 1000\ pa$
$\rightarrow \gamma = 1500\ \frac{kg}{m^3}$

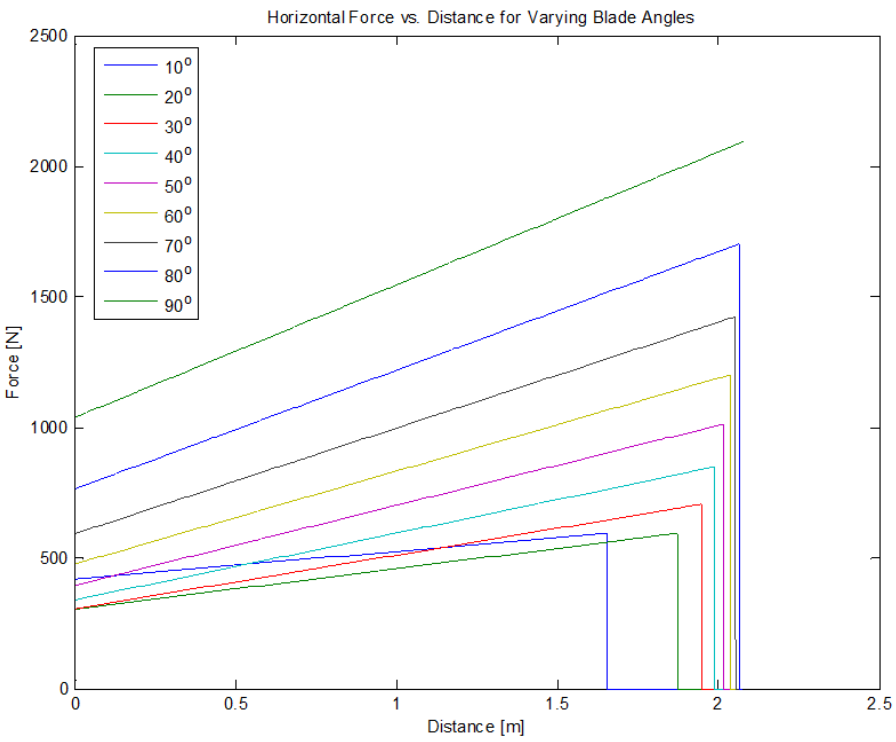


Figure 4: Forces for Varying Blade Angles at 15cm

Figure 4 shows the horizontal force on a blade over the swipe distance for varying blade angles. Stewiacke soil was used for this simulation so that the results could be compared with published results. The resulting forces agree with published results for both modeling and

experimental results [4]. It can be seen that most of the blade angles are able to travel close to two meters before the maximum volume is reached, but the horizontal force on the blade varies drastically. A sharp blade angle of 20 degrees would reduce the required force four fold when compared to a 90-degree blade, without requiring a large decrease in total volume moved per swipe. This would imply that a sharp blade angle would be optimum, but this does not hold for all cases.

Figure 5 shows that by increasing the cutting depth from 15 to 35 cm, there is a drastic change in the simulation due to the heavily increased cost to engage for sharp blades.

$\rightarrow \varphi = 30°$

$\rightarrow \delta = 15°$

$\rightarrow w = 25.4\ cm$

$\rightarrow v = 1\ \frac{m}{s}$

$\rightarrow \underline{d = 35\ cm}$

$\rightarrow h = 75\ cm$

$\rightarrow C = 2000\ pa$

$\rightarrow C_a = 1000\ pa$

$\rightarrow \gamma = 1500\ \frac{kg}{m^3}$

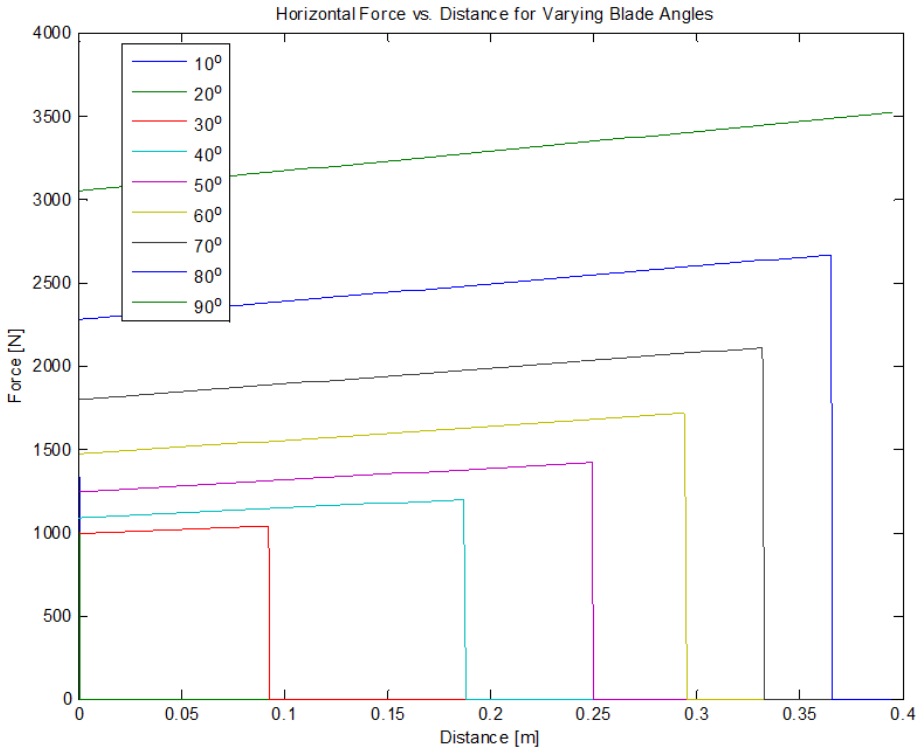


Figure 5: Forces for Varying Blade Angles at 35 cm

The figure shows that the increase in cutting depth greatly changes the tradeoff between volume per swipe and horizontal force. When comparing the 90-degree and 60-degree blades, the sharper blade would half the horizontal force required to doze, but would also decrease the maximum volume by over 25%. These two simulations show that a small change, such as the cutting depth, can greatly affect the optimum blade choice. With this in mind, an optimization was built to generate the best blade angle for a given set of parameters.

### *2.2.2 Optimization*

Three metrics were developed to build a cost function for the optimization. The first metric was the power efficiency of the dozer.

$$PowerEfficiency = \sum \frac{Material\ Dozed}{Power\ Input} = \sum \frac{\gamma V_{max}}{Hv}$$

The power efficiency is a calculation of the material moved per given power input. A graph of the power efficiency is shown below in Figure 6. The blade angle is varied between 0 and 90 degrees and the speed range is 0.5 m/s to 2 m/s, the operational range of the robot. The third axis is the normalized value of the power efficiency in units of kg/watt. The plot shows that the greatest power efficiency is achieved at the lowest possible speeds because of the velocity term in the denominator of the equation. In order to counter act this inclination for lower speed the next metric, time efficiency was developed.

The Time efficiency is a calculation of the material dozed per time with units of kg/s.

$$TimeEfficiency = \sum \frac{Material\ Dozed}{Time} = \sum \frac{\gamma V_{max}}{(l_{max}/v)}$$

It is interesting to note that the normalized time efficiency, Figure 6 below, is a linear function of velocity because $V_{max}$ and $l_{max}$ have the same behavior.

The final metric was max volume dozed per swipe. This metric is important because the greater the displaced volume per swipe of a given blade design the fewer number of swipes needed to clear an area.

$$Volume = \sum Material\ Dozed = \sum \gamma V_{max}$$

This metric normalized can be seen below in Figure 6; it has units of $m^3$ and is only a function of blade angle. These normalized metrics were then weighted and summed to form a cost function for the given situation. This is shown in the equation below.

$$Cost = c_p(PowEff) + c_t(TimeEff) + c_v(Vol)$$

An example of the individual metrics and the final cost function can be seen below in Figure 6. The weights of $C_p = 0.5$, $C_t = 0.2$, and $C_v = 0.3$ were used. This selection is based on the assumption that when using robotic dozing the power efficiency was most important because of battery consumption.

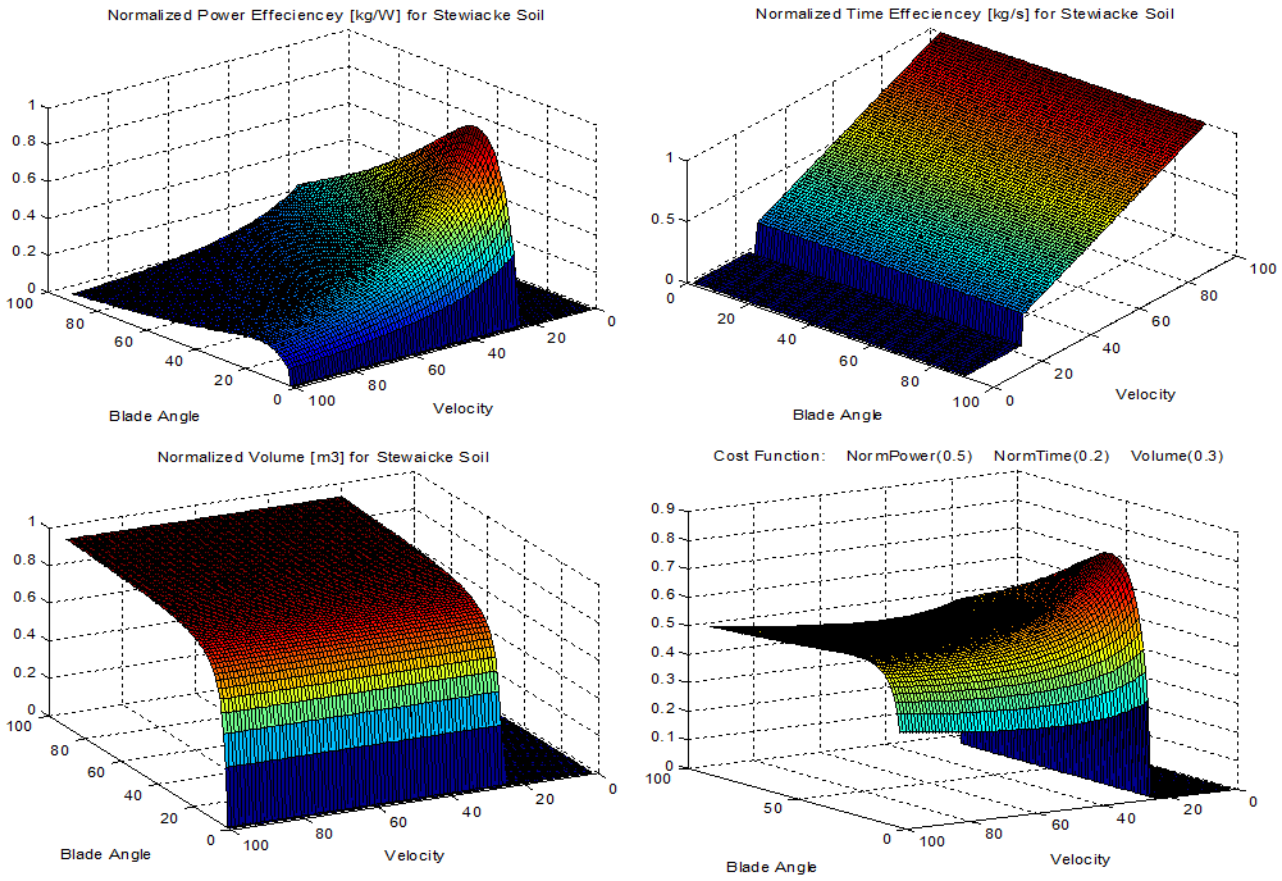


Figure 6: Individual Metrics and Overall Cost Function for Blade Angle Optimization

For all cases, the cost function turns out to be a saddle point with no global optima. This means that the dozing should be done either as slow or as fast as possible depending on the weights of the metrics. This is an unexpected result, because the goal was to generate an optimum angle and speed for every situation. Based off this result, instead of looking for an optimum velocity and angle, the optimization was built so that it integrated the cost function for each given blade angle, over the operational range of speeds. The angle with the greatest value is determined to be the optimum angle for the given set of conditions and speed range. This calculation is shown below

$$max\left(\int_{v_{min}}^{v_{max}} cost(\alpha)dv\right) \quad for\ 0 < \alpha\ < 90$$

For the first simulation shown in the previous section with d = 15 cm, the integration over the speed range is shown in Figure 7. The max value of this integration is 21 degrees.

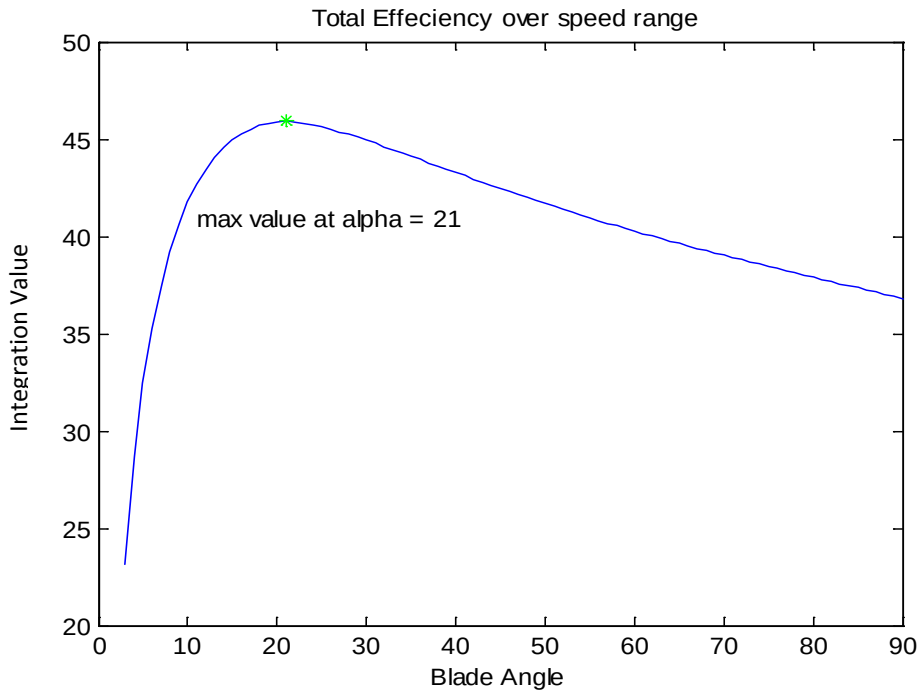


Figure.7: Optimum Angle at 15 cm

As expected from the previous discussion in the simulation section, increasing the cutting depth to 35 cm has a drastic effect on the optimum angle. Figure 8 shows how this increase in cutting depth greatly increases the optimum blade angle from 21 to 90 degrees.

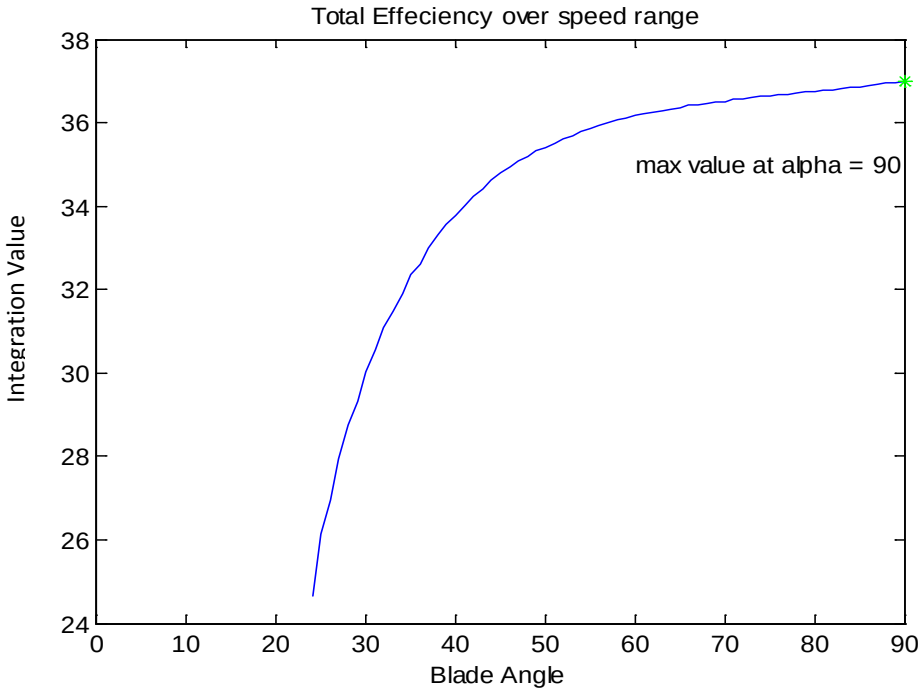


Figure 8: Optimum Angle at 35 cm

The optimization results show that the blade design is highly dependent on the conditions and can vary over a large range of angles. Because of this result, a variable angle blade design is proposed in Section 4.1 to increase the efficiency of the dozing operation. It should be noted that changing the weights on the cost function can have a large effect on the resulting blade angle. The weights used in the presented example reflect a scenario where battery consumption dominates; therefore the power efficiency is weighted highest. If path planning algorithms were being used to complete dozing jobs, the volume metric would most likely be increased in order to reduce the total number of swipes required. Real world use of this optimization will require great consideration of the tradeoffs between speed, power efficiency, and swipes required.

## 2.3 Discussion

This chapter explained a common method for blade-soil interaction and expanded this model to include the dynamic effects of dozing and a volumetric analysis. Using this model a MatLab simulation was created which outputs the vertical and horizontal forces on a dozing blade for varying blade angles, soil properties, and cutting depth. From this simulation it was found that varying the attack angle of a blade can greatly influence the forces on the blade. Because of this, three cost function metrics were created to optimize the blade angle. This optimization is demonstrated for varying the cutting depth of a dozing operation and could be used for varying soil parameters as well. In addition, if a user has fixed dozing blade this optimization could be easily adapted to solve for the optimal cutting depth which would be advantageous for path planning purposes.

From these results, it was determined that a variable angle blade could greatly improve dozing performance. This leads to a new blade design which is demonstrated in Section 4.1. A model combining the new blade, the dozing forces, and the robot model shown in Chapter 3, is built and tested in Chapter 4.

# 3 Suspension Study

In the previous chapter the effect of blade geometric design on dozing performance was analyzed and the relationship between the physical design and operational parameters was discussed. In this Chapter the effects of suspension configuration on overall dozing performance is investigated. The analysis focuses on six-wheeled vehicles using independent wheel suspensions and independent motors.

As previously noted, the increase in mobility achieved by wheeled vehicles comes at a cost of overall traction. Further complicating the issue with six wheeled vehicles is the uneven contact force distribution throughout the wheels. Figure 9, which shows the current distribution to the six wheels of a dozing robot during flat ground testing, highlights this issue. The figure shows that the front wheels draw the most current (therefore apply the most torque), followed by the rear wheels, and lastly the middle wheels supply the least torque. This uneven torque distribution can cause poor handling of the robot, underperformance in push and pull situations, and unpredictable slip of the wheels. If the torque distribution of the wheels can be equalized, then the overall performance of the robot can be increased significantly.

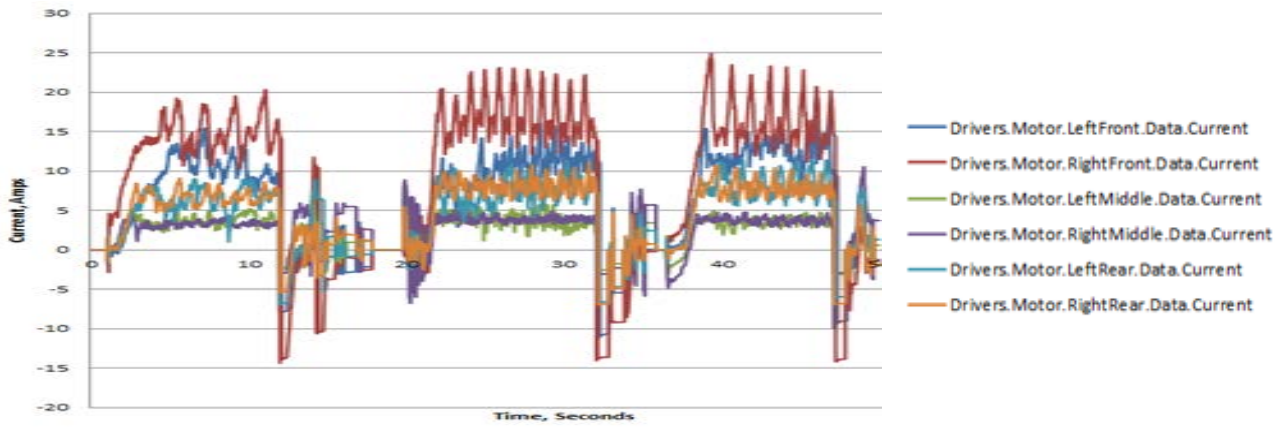


Figure 9: Current Draw for 6x6 Robot

One increasingly popular solution for torque distribution problems is active torque vectoring control. Torque vectoring techniques allow for independent control of the torque applied by each wheel and allow a controller to guarantee each wheel is applying similar torques. While this can be a good solution for 4-wheeled vehicles where the weight distribution is more likely to be equal, torque vectoring is not easily able to adjust the normal force distribution. Therefore, torque vectoring would require a drop in applied torque to the front and rear wheels to achieve equalized torques in a 6-wheeeled robot. This study takes a different approach by investigating the potential of using an adjustable suspension system to help increase the performance of the dozing vehicle. Instead of adjusting the torque directly, implementing an adjustable suspension would adjust the normal force of each wheel which would help to equalize the applied torque indirectly.

In order to test the benefits of a semi-active suspension system, simulation backed by experimental validation was used to evaluate the promise and value of such a design in light dozing applications. In addition to the suspension study, building a full robot model allows for easy adaption for future design or sensitivity studies. Three simulation packages were evaluated for use and SimMechanics was chosen. Following the selection of the simulation package, a full model of the robot was built and a semi-active suspension system was studied. This includes the experimental validation of the model and optimization of the suspension.

## 3.1 Vehicle Model

SimMechanics was chosen to build the vehicle model because it was designed to be used for kinematic simulations of multi-body systems [8][9][10] and it has many advantages over similar software packages. It is simple to import CAD models into the SimMechanics interface directly from CAD software. In addition, the block based programming is easy to learn and gives the user complete control of all aspects of the model. In this way, the model can be defined as simple or complex as the study requires. Finally, it is simple to collect the pertinent data and the seamless interface with MatLab allows for easy data analysis and control.

The robot being studied is a 6x6 pivot-arm-suspension experimental robot currently used for mapping operations. As previously mentioned there is interest from industry to adapt this robot for dozing operations which would require greater performance in terms pushing ability and resistance to slip. The robot is shown below in Figure 10. A simplified kinematic breakdown of the robot and the constraints applied is shown below in Figure 11.

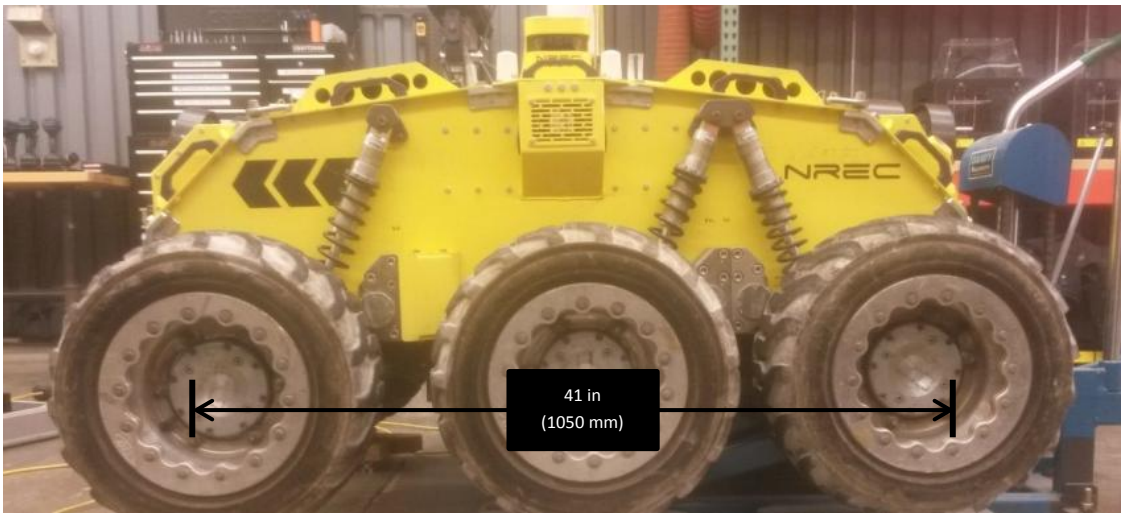


Figure 10: Robot Being Studied

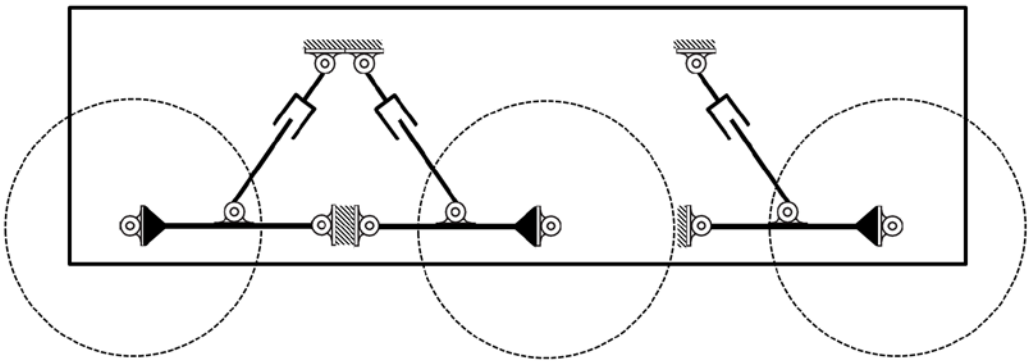

Figure 11: Kinematic Breakdown

The major subsystems which influence the study include the wheels, swing arms, suspension spring and dampers, and the vehicle hull. Figure 12 illustrates these components, the hull is shown in yellow, the female spring and damper component is shown in red, the male component is shown in orange, the swing arm is shown in black, and the wheel is shown in grey. Each wheel is independently driven by in-hub motors, but for simplicity this geometry is combined with the swing arms. To begin building the model a simplified version of the robot was built in CAD. These components maintain the structure and shape of the actual robot components, but only require that the center of mass, inertias, and overall weight be the same. This can be done by importing these values from the complete CAD model and manually overriding the values for the simplified components.

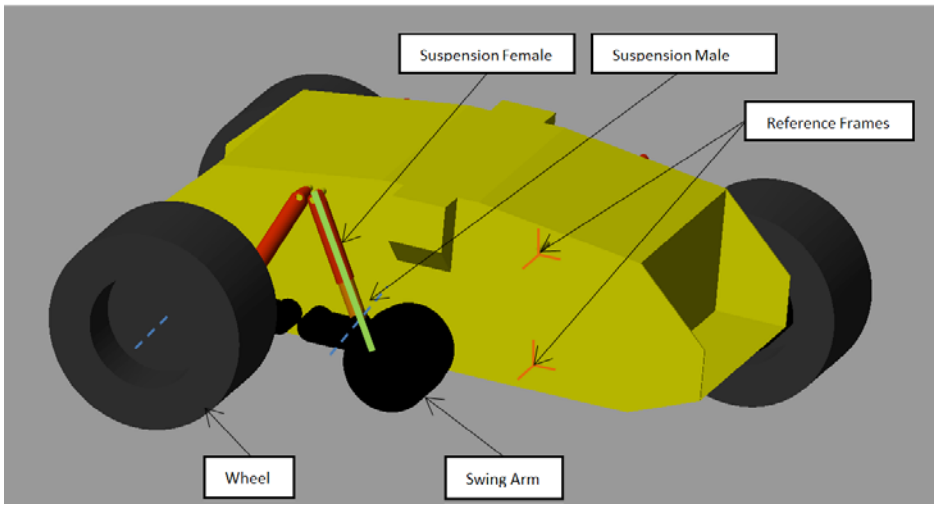


Figure 12: Robot Components and References

First, the hull was imported and reference frames were placed at the 6 connection points on each side of the hull. This is shown by the two orange Cartesian frames on the right side of the robot illustrated in Figure 12. The SimMechanics code for the robot is shown in Figure 13,

the hull is highlighted in yellow and each of these reference frames is a line stemming from the hull. Once the reference frames were placed it allowed for easy construction of the constraints. The swing arm and suspension assembly is simplified into one block in Figure13, highlighted in blue and the contents of this block are shown in Figure 14. One side of the swing arms, highlighted in red in Figure 14, was constrained with a revolute joint, denoted Revolute9 and highlighted in brown, to the hull via the lower reference frames. Below the rotational joint is a hard stop which imposes limits on the rotation of the swing arms. Next, the tires, green boxes in Figure 13, were constrained to the swing arms with a revolute joint, illustrated by the dashed blue line on the left side of Figure 12 and as Revolute1 highlighted in pink in Figure 14, which allowed the tires to rotate in reference to the swing arms. As noted earlier, the motors are combined with the swing arms, therefore the tires can be actuated by simply demanding a rotational speed/position to the rotational joint connecting the swing arms and wheels. This could be expanded to include electric/motor/torque models, but was out of the scope of this project.

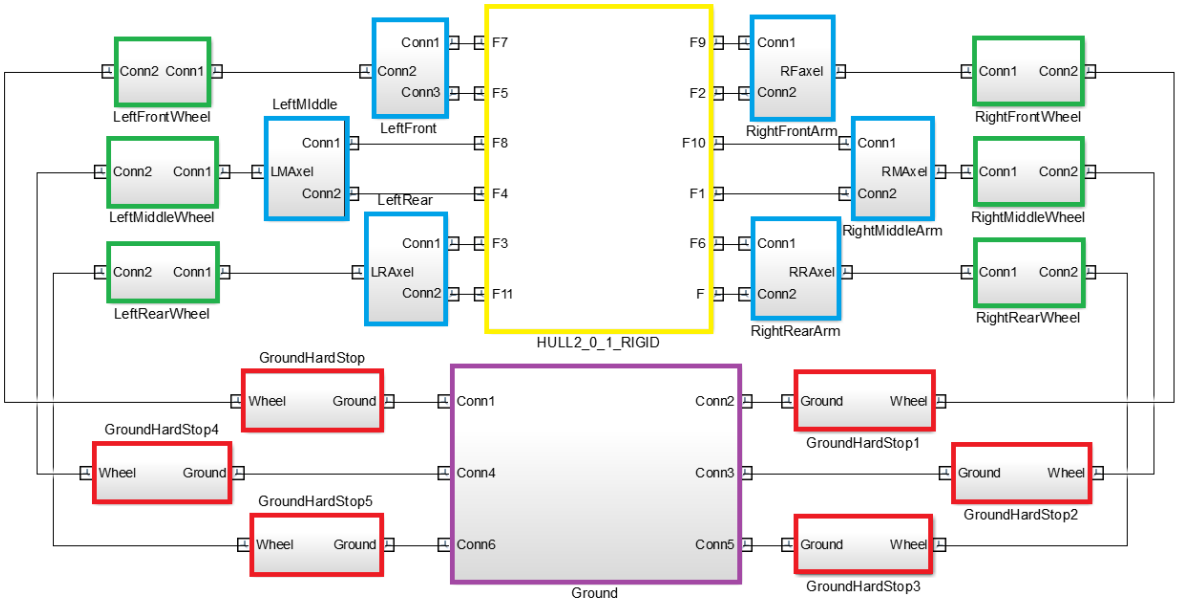


Figure 13: SimMechanics Code of Robot

The complete spring and damper modules were slightly more complex to model. The top of the female spring and damper component was constrained to the hull by a revolute joint, denoted Revolute2 in yellow in Figure14, at the top reference frame. This constraint alone would allow female component to rotate freely in reference to the hull. The male component was constrained to the to the swing arm by a cylindrical joint whose axis is shown in the middle portion of Figure 12with a dashed blue line and denoted Cylindrical9 in black in Figure14. A cylindrical joint was used in order to place the joint properly, but it is constrained along the sliding axis and can be thought of as a revolute joint. Next, the male component was defined to

slide inside the female component via a prismatic joint illustrated by the green line in the middle portion of Figure 12 and shown as Cylindrical3 in green in Figure14. SimMechanics allows for spring and dampers to be applied to all constraints so it was simple to apply the correct spring stiffness and damping coefficient to the prismatic constraints inside the suspension. Shown in Figure14 is a custom spring and damping module which was added and is discussed in the next section.

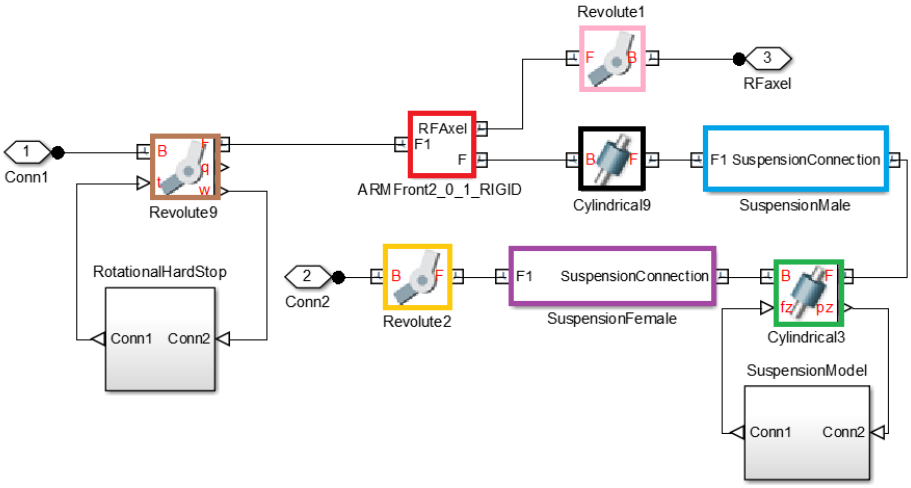


Figure 14: Swing Arm and Suspension Code

For the basic model the ground is simply an immovable slab. The environment can be made simple (this case) or can be expanded to be more representative of real world situations. An example of a more complex environment is demonstrated in Chapter 4 of this thesis. Each wheel is constrained to have a simple point contact hard stop with the ground and the interaction is defined with spring and damping coefficients. The ground is defined and highlighted in the purple box in Figure13 and the ground contact hard stop is defined in the red boxes. More complex ground contact models could be employed in SimMechanics (e.g. ground contact patch, slip, tire pressure, etc.) [11] , but were not necessary for the suspension study and therefore fell outside the scope of this project. The full completed model is shown below in Figure 15.

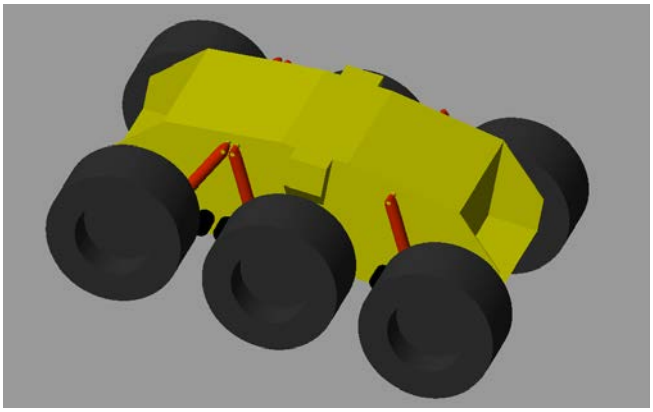

Figure 15: Completed Model

## 3.2 Suspension Study

### *3.2.1 Model Verification*

As previously discussed, if the normal force distribution among the six wheels can be equalized then the handling, mobility, and tractive force can be increased. The robot in this study has an adjustable suspension such that the pre-load or rest position of the suspension can be adjusted. This adjustable suspension is shown in Figure 16. The SimMechanics model was easily adjusted so that varying pre-loads can be simulated. This added model is shown in Figure14 in the block labeled SuspensionModel. The goal of this study is to first, validate the simulation with physical testing, and second to find the suspension pre-loads which equalize the normal forces for the robot for different situations.

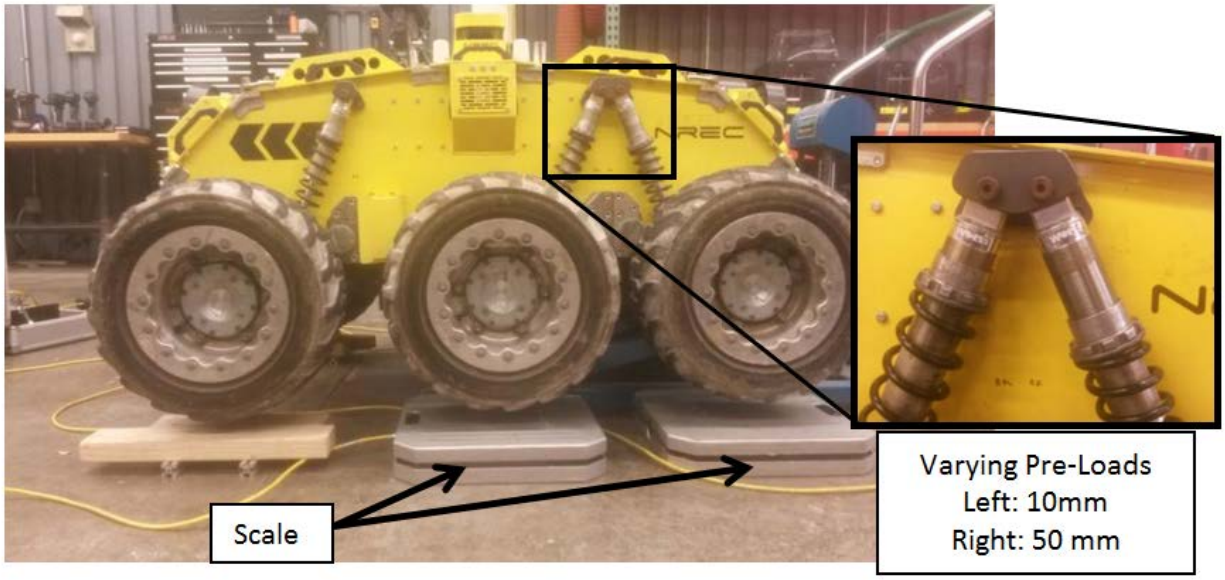


Figure 16: Lifter Robot Over Scales with Varied Pre-Loads

In order to validate the simulation, experiments with the robot were completed. First, the robot was lifted off the ground and the suspensions were set to different pre-loads, the difference in pre-loads is highlighted in Figure 16. Next, scales were placed under each wheel and the robot was lowered to the ground. The normal force for each wheel was recorded. It was found that the suspension was quite stiff due to internal friction so, in an attempt to overcome this, each tested suspension pre-load was repeated with added weight on the robot. 250 kg was added to the robot to increase the overall weight of the system by ~50%. The robot with this added weight can be seen in Figure 17. These tests were completed for 4 different suspension configurations, for a total of 8 different tests.

Figure 17: Robot with Added Weight

Following the physical testing, simulations for each configuration was run in SimMechanics. An image of the simulation with the added weights is shown in Figure 17. The comparison of these results is shown below in Table 1. It should be noted that the simulation assumes symmetry for the normal force distributions from side to side (i.e., left front wheel will have the same load as right front wheel), this held true during the physical experiments therefore; an average between each side is presented.

To validate the simulation based on the test results there are two important criteria to consider. First, the percent difference between the testing and the simulated normal force values gives an indication of how accurate the model is. Secondly, the correct ordering of the magnitudes of normal forces (i.e., the front wheel has the largest force, then the rear wheel, and the middle wheel has the lowest force) gives confidence in using the model for prediction. This is because the goal of the model is to change the suspension configuration in order to increase or decrease the normal force on a particular wheel. In most cases the percent difference is relatively low and the few large values can be explained by experimental error. The simulation uses an ideal spring and damping model, but as previously noted, the suspension system had a lot of internal friction and did not behave ideally. In addition to low percent differences, the majority of simulation cases correctly predicted the ordering of the magnitudes of normal forces. For example, even for one the worst cases in terms of percent difference, weighted test 2, the model still correctly predicts that the middle wheel will have the lowest normal force, followed by the front, and lastly the rear will have the greatest normal force.

Table 1: Validation Results

| | | | Physical Testing (lbs.) | | Simulated (lbs.) | | Percent Diff. | |
|---|---|---|---|---|---|---|---|---|
| Test | Wheel | Preload (mm) | Unweighted | Weighted | Unweighted | Weighted | Unweighted | Weighted |
| 1 | Front | 50 | 228 | 298 | 217 | 306 | -5.3 | 2.8 |
| | Middle | 10 | 107 | 225 | 138 | 231 | 22.4 | 2.8 |
| | Rear | 50 | 244 | 329 | 213 | 310 | -14.4 | -6.1 |
| 2 | Front | 50 | 210 | 317 | 205 | 292 | -2.8 | -8.7 |
| | Middle | 10 | 142 | 160 | 152 | 254 | 7.0 | 37.2 |
| | Rear | 10 | 228 | 377 | 211 | 302 | -8.3 | -24.9 |
| 3 | Front | 10 | 172 | 292 | 163 | 252 | -5.8 | -15.9 |
| | Middle | 50 | 210 | 228 | 240 | 332 | 12.5 | 31.5 |
| | Rear | 10 | 194 | 333 | 165 | 263 | -17.7 | -27.0 |
| 4 | Front | 10 | 188 | 289 | 209 | 294 | 10.3 | 1.7 |
| | Middle | 10 | 180 | 269 | 156 | 258 | -16.8 | -4.0 |
| | Rear | 50 | 208 | 297 | 202 | 294 | -3.3 | -0.8 |

The majority of tests yield promising results, with only one case which produced poor results. The weighted test for configuration 3 has both a high percent difference and does not correctly predict the normal force ordering. As previously noted the suspension had a large amount of internal friction which was not accounted for in the ideal SimMechanics model. To account for this and make the model more realistic, each suspension model could be individually tested and characterized.

### *3.2.2 Suspension Optimization*

With the vehicle model validated via experimentation, the next investigation examined how the normal force distribution could be equalized by changing the suspension configuration. Equalizing the normal force can increase the handling of the robot and increase the forward thrust for dozing. To achieve this goal an optimization to calculate the best suspension configuration was created. Many optimization techniques may be appropriate for a given scenario, but a modified depth first search optimization technique was chosen to accommodate the many possible configurations and scenarios the model can have. For example, this technique could accommodate losing any one or more wheels and still produce the best suspension configuration to equalize the normal forces.

The optimization works by having MatLab code set the preload of the wheels and then call the SimMechanics simulation which returns the steady state value of the normal force values. The MatLab code then systematically adjusts the preloads by a predetermined step size

until the best, most equalized, normal force distribution is found. The initial step size is determined such that the full scope of pre-load positions is covered. For example, starting at 0 mm and using five 22.5mm steps would cover the full scope of possible pre-loads (max of 112 mm for this particular robot). Then the step size is decreased and the process is repeated with a narrower search field, now centered about the previous solution. This decreasing of step size and search field is continued until a solution with desired precision is found. By narrowing the search field and decreasing the step size an exhaustive search of all possible combinations was avoided. For some test cases an exhaustive search was performed and the optimization was found to converge to the same solution.

This technique is illustrated with a step size of 45mm in Figure 18 below. First, the front pre-load is set, in this case to 45 mm, and then the middle pre-load is set to 0 mm. Next, the rear pre-load is varied from 0-45-90 mm. Then the search backtracks and sets the middle pre-load to 45 and repeats the rear pre-load setting. This pattern is continued for all middle pre-load values, and then backtracks again to reset the front pre-load value.

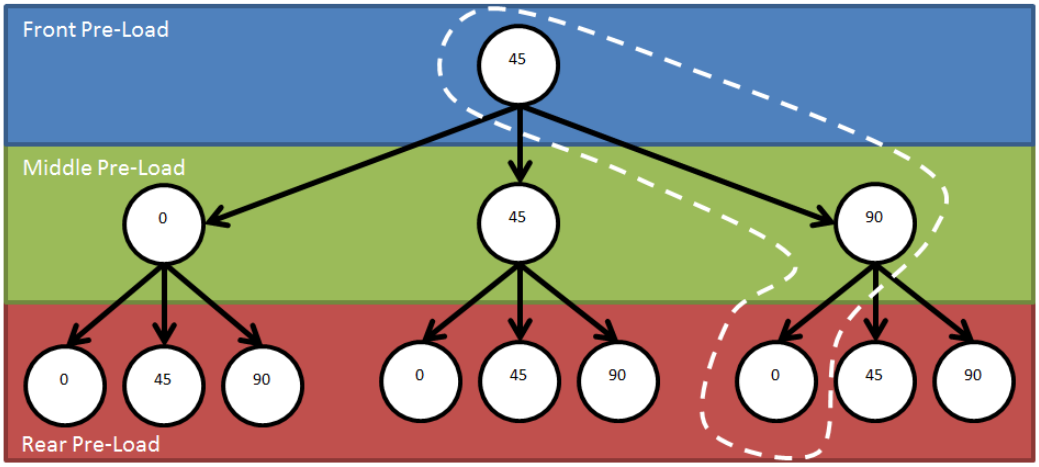


Figure 18: Search Procedure

Once the best configuration is found for a given step size, this procedure is repeated with a smaller step size. For example, if the optimal suspension configuration for a step size of 45 mm was 45-90-0 (circled in dashed white in figure 18), the next iteration would expand with a smaller step size around these points. The next iteration would test 22.5-45-67.5 for the front pre-load, 77.5-90-112.5 for the middle, and 0-22.5-45 for the rear. Note that the pre-load cannot be negative so the search would look expand to the positive side of zero. Similar iterations would be completed until an acceptable solution is found.

With the simulation and optimization completed the optimal suspension configuration can now be found for any given scenario. The next chapter presents example test cases which show application of this optimization.

## 3.3 Discussion

In this chapter a model of the vehicle being studied was presented. This model, built in SimMechanics, was a simplified version of an actual robot while maintaining all the kinematic and physical properties. The model was then verified through physical experiments. Following acceptable model verification, an optimization for the optimal suspension properties was created. This program searches and finds the optimal suspension pre-loads for any given scenario. The model and optimization will be expanded to include a variable angle blade discussed in the second chapter. This combined model and example cases are found in the next chapter.

# 4 Combined Model

Chapter 2 showed how the creation of a variable angle blade design could increase the efficiency of dozing operations. Chapter 3 demonstrated how a vehicle model and optimization could be used to find the optimal suspension configuration for a given operating scenario. This chapter contains a combination of both of these studies. A new blade design is created and then built in SimMechanics. This new design is then coupled with the existing vehicle model to create a complete model of wheeled vehicle dozing. This new model is run for various operational scenarios and shows an increase in dozing performance for the vehicle.

## 4.1 Blade Design

Given the results of the optimization in section 2.2.2, which shows the need for a variable blade with a large range of possible attack angles, a new blade is proposed. This new blade design consists of a two part blade, shown in blue in Figure 19, which can vary the attack angle from 0-90 degrees. The lower blade is connected to the robot, represented by the yellow body, by two rotational joints in series with a prismatic joint. The top is connected by a solid body with a rotational joint on each end. The kinematic breakdown for the design is shown in Figure 19. This design contains three degrees of freedom which could be actively controlled or the joints could be designed so that preset angles (e.g., 15, 30, 45, 60, 90) could be locked in manually.

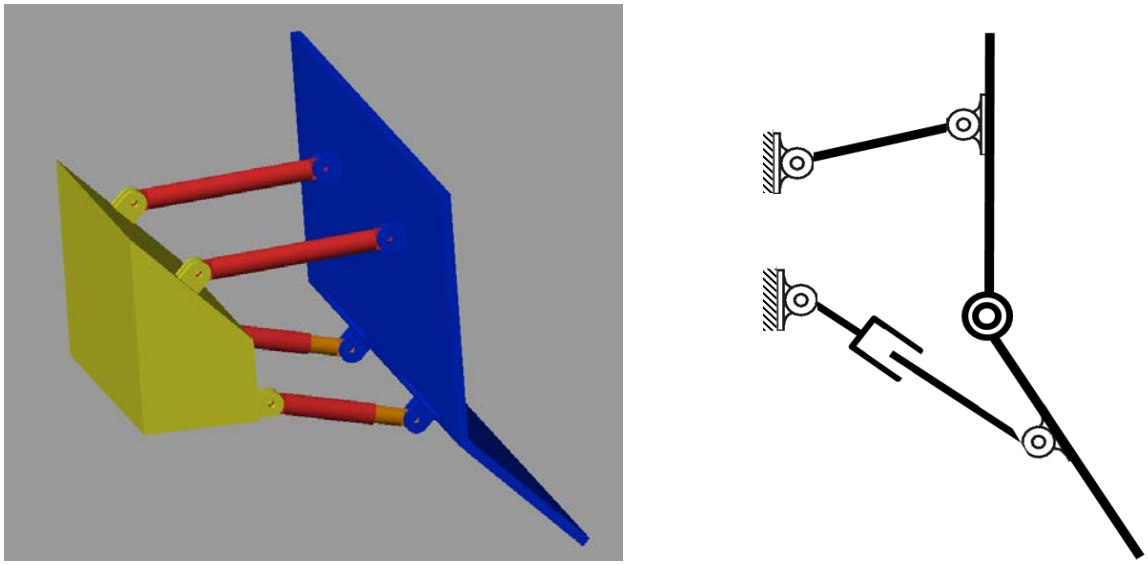

Figure 19: Variable Angle Blade Design

## 4.2 Updated Model

The vehicle model presented in 3.1 was combined with the blade design presented in section 4.1. The SimMechanics code for this combined model is shown below in Figure 20. The vehicle model which was shown in Figure 13 is now contained in the brown box in Figure 20. Connected to the vehicle model is the blade model, which is contained in the Green box. This blade model, which is pictured in Figure 19, connects to the robot through the top and bottom ports labeled BladeConnection and a. With only these connections to the robot, the blade model would have no knowledge of the ground configuration. Therefore, the ground definition is connected to the blade model through a hard stop shown highlighted in Blue. Finally, the dozing forces model presented in 2.2 is called in the red box labeled Forces.

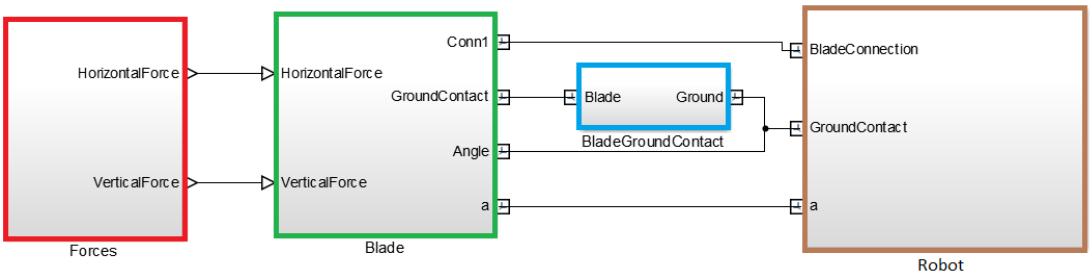


Figure 20: SimMechanics Code for Combined Model

To begin, the user inputs the desired dozing parameters and suspension configuration. Then, the blade-soil interaction model is called and determines the horizontal and vertical forces to place on the blade. Next, the blade angle optimization code is run and determines the optimal angle for the dozing blade. This is all done outside of SimMechanics in separate MatLab code and then imported into the workspace automatically. To complete the initialization, the blade is set to the optimal angle, placed in contact with the ground, and then all of the joints are locked. This would be similar to a dozing blade being adjusted before a job and then locked into place.

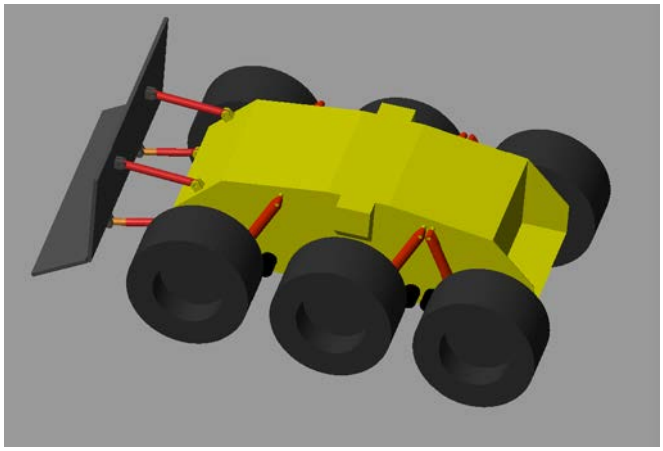

Figure 21: Combined Model

A picture of the initialized simulation can be seen in Figure 21 above. SimMechanics will attempt to import constraints settings not pre-set at steady state, but is not always successful. Therefore, to begin the simulation, the robot is at rest for a short amount of time until it reaches steady state. Once the simulation has been allowed to settle, the forces are applied to the blade, which is transferred through the connections with the robot and to the ground. The wheels apply an opposing force to the ground proportional to the amount of normal force which is seen by the wheel.

This model was used to evaluate the optimal suspension under dozing conditions. Example cases are presented in the next section. First, the optimal solution for forward driving is compared to the optimal solution for dozing forward. Next, the same test is repeated for driving the robot in reverse with the dozing blade placed on the back end of the robot. These two tests highlight the effectiveness of a semi-active suspension and show a large decrease in the normal force distribution. Finally, a vibration table is added to the simulation and a simple suspension tuning study is run. This example highlights the flexibility of building a complete model and shows how such a model is easily adaptable to many different types of studies.

## 4.2 Example Cases

### 4.2.1 *Forward Driving & Dozing*

The simplest scenario which the robot will be operating is forward driving without any dozing forces applied. The optimization was run and it was found that optimal suspension configuration was to have all pre-loads set equal to 22.5 mm. The normal forces are almost equal for this configuration and are tabulated in Table 2. This suspension configuration, all pre-loads equaling 22.5 mm, was set in the simulation and run with the dozing forces applied to the blade. As expected, the normal force distribution changed drastically when a horizontal and vertical force was applied and is shown in Table 2.

The suspension optimization was run again, this time with dozing forces applied. The optimal configuration for dozing on flat ground was found to be front pre-load = 106.8, middle pre-load = 95.6, and rear pre-load = 78.8. These results are included in Table 2 below. For comparison this suspension configuration was then run under the flat driving conditions. The driving normal force are affected very little by the uneven suspension pre-loads, therefore if the robot was only used for forward dozing and driving this suspension configuration could be set and not changed.

Table 2: Flat Driving & Dozing Comparison

| Configuration | Wheel | Pre-load (mm) | Driving Normal Force (lbs.) | Dozing Normal Force (lbs.) |
|---|---|---|---|---|
| 1 | Front | 22.5 | 189.7 | 235.2 |
| | Middle | 22.5 | 190.4 | 187.9 |
| | Rear | 22.5 | 190.8 | 172.0 |
| 2 | Front | 106.8 | 187.7 | 213.9 |
| | Middle | 95.6 | 193.1 | 201.8 |
| | Rear | 78.8 | 189.5 | 180.2 |

Equalizing the ground reaction forces has two performance benefits for wheeled robots. First, with an even distribution of forces the robot will have increased handling, mobility, and controllability. Secondly, the normalization of the reaction loads will increase the overall dozing ability of the robot. The applied force of each wheel has to be less than the maximum frictional force or else slippage will occur:

$$F_{applied} \leq \mu F_{normal}$$

Assuming that the coefficient of friction is large enough, the maximum force each wheel can apply is proportional to the normal force of that wheel:

$$F_{applied} \propto F_{normal}$$

The sum of the normal forces is not changing for any given suspension configuration, therefore the total push force generated does not increase by equalizing the normal force distribution. The benefit of this equalized distribution is achieved at high loading, when the motors reach their torque limits. Using the dozing case presented above with configuration 1, the front wheel will apply 40% of the total forward push force. Under high loading conditions this motor will reach its torque limit well before the other wheels. Therefore, by reducing the front normal force by 10% when switching to configuration 2 the total force that can be applied by the front wheel before the motor limit is reached is increased by 10% as well.

### *4.2.2 Reverse Driving & Dozing*

Given the asymmetric suspension configuration of the robot, a simulation reversing the driving and dozing direction of the robot was completed. The simulation allowed for easy transfer of the blade to the rear end of the robot and the dozing forces and driving direction was easily changed. An image of the simulation with the dozing side reversed can be seen below in Figure 22. The same tests as the previous section were run and are presented in Table 3 below.

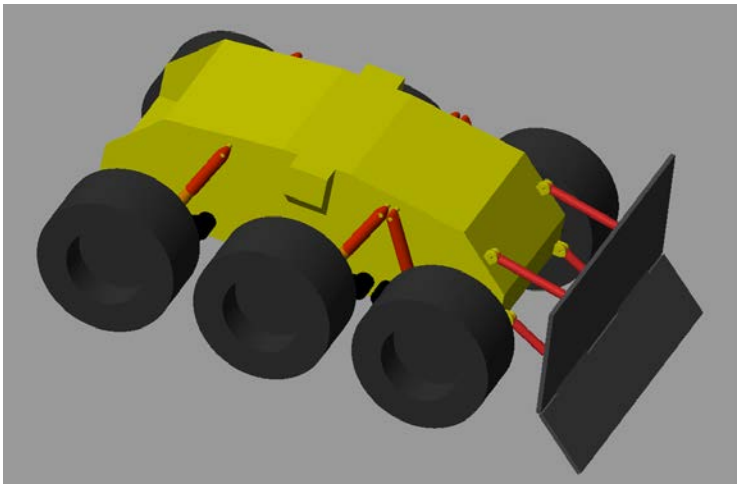

Figure 22: Reverse Driving and Dozing

Table 3: Flat Driving & Dozing in Reverse Comparison

| Configuration | Wheel | Pre-load (mm) | Driving Normal Force (lbs.) | Dozing Normal Force (lbs.) |
|---|---|---|---|---|
| 1 | Front | 22.5 | 189.7 | 160.9 |
| | Middle | 22.5 | 190.4 | 172.2 |
| | Rear | 22.5 | 190.8 | 244.4 |
| 2 | Front | 73.1 | 192.7 | 186.2 |
| | Middle | 78.8 | 182.8 | 191.2 |
| | Rear | 95.6 | 192.0 | 203.9 |

The data shows (using the same logic presented for forward driving/dozing) that the optimal suspension configuration can increase the maximum forward force by the rear wheel by 16%. This increase in ability and the spread of normal forces is better than the forward dozing configuration, therefore the robot should operate in reverse when conducting dozing operations. Again, the driving normal force is only slightly affected by the uneven suspension configuration, therefore if the robot was only used for reverse driving and dozing this configuration could be set and left unchanged.

### *4.2.4 Suspension Tuning*

Following the study of a semi-active suspension presented previously, a simulation for suspension tuning was created. This simulation placed the robot on a suspension tuning table with six independently movable pistons and tested the suspension response under various conditions.

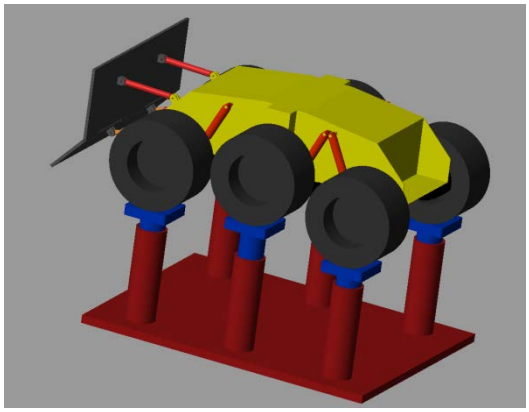

Figure 23: Suspension Tuning Table

Presented below is the system response to 1 Hz sine wave with amplitude of 7 cm being output by the pistons. This sine wave represents the robot driving with bumpy ground conditions. The different lines plotted in Figure 24 show how the hull center of mass position and acceleration changes with varying spring and damping coefficients. These results and similar testing could be used for a design study which tunes the suspension for various operations and highlights the benefits of building a complete SimMechanics model of the vehicle.

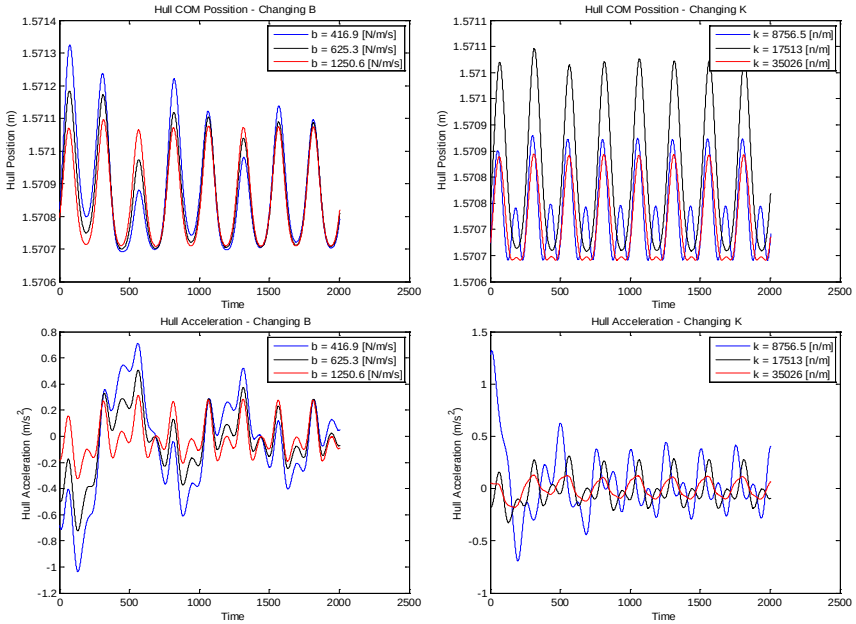


Figure Suspension 24: Tuning Results

## 4.4 Discussion

This section demonstrated the combination of blade angle optimization and suspension optimization. From the analysis of the dozing forces a new variable angle blade design was presented. This model was then combined with the full vehicle model for a complete dozing simulation. This simulation was run for two dozing example cases and shows that the optimal suspension configuration can greatly equalize the normal force distribution on the wheels. In addition a suspension tuning example is presented which highlights the benefits of building a complete vehicle model.

The results for the dozing example cases show promising results for dozing performance. First, the decrease in variation of normal force distribution will increase the handling, mobility, and controllability of the robot. Next, it was shown that the suspension optimization could increase the maximum applied force for both forward and reverse dozing. Finally, the simulation showed that the normal force distribution is better for the reverse dozing condition and therefore, dozing operations should be conducted in reverse. The vehicle kinematics could be explored to explain this, but it seems that the normal force distribution benefits front the pair of asymmetric suspension arms being closer to the applied loads.

# 5 Conclusion

## 5.1 Summary and Conclusion

This thesis presented an exploration of wheeled robotic dozing and potential ways to improve upon vehicle performance. To begin, soil dozing models were explored and a simulation of dozing forces was created. This simulation was then used to optimize the blade angle for a given set of dozing conditions. A new blade design was proposed which would allow for the blade angle to adjust from 15-90 degrees. Following the study of the blade design, the suspension of the vehicle was evaluated. In order to test different suspension configurations a full vehicle model was created in SimMechanics. This model allowed for various simulations to be run and pertinent data to be collected. This simulation was then used to create an optimization program which found the best suspension configuration for a given set of operating parameters. Finally, the dozing model presented in the second chapter was combined with the full vehicle model in the fourth chapter to create a full vehicle dozing model. This model was used to find the optimal blade angle and suspension configuration for dozing operations.

This work has shown that a variable angle blade can improve the performance of a dozing robot. By using the optimization presented the blade angle can be determined in order to optimize the dozing operation in terms of power, volume, and/or time efficiency. This system could be beneficial to dozing operations and increase the effectiveness of small scale dozing. . For shallow dozing, this a variable angle blade can reduce the overall push force required up to 75% while reducing the total volume per swipe by only 15%. In addition to the blade design, the semi active suspension was shown to be able to increase the dozing performance. If using the recommended reverse dozing configuration, the overall push force can be increased by 16%. In addition to the push force, finding the optimal suspension configuration which equalizes the ground reaction forces can increase the robots handling, mobility and controllability.

## 5.2 Contribution

The contribution of this work has four main components. First, an analytical framework, metrics, and optimization were developed to compute the optimal blade angle for dozing operations. This new blade design has the potential to greatly increase the efficiency of dozing operations. Second, based off the analysis, a new variable angle blade design was created. Thirdly, a framework and optimization for estimating the optimal suspension parameters to maximize ground reaction was developed. This semi-active suspension has the ability to help equalize the normal force distribution for wheeled vehicles and increase overall performance in many operational scenarios. Finally, the fourth contribution is the demonstration of full vehicle simulation using SimMechanics. Building the model in SimMechanics has a wide range of applications and is easily customizable. Together, these components help to understand the value and limitations of dozing with wheeled vehicles and show promise to increase the overall system effectiveness.

## 5.3 Future Work

Future work on this topic should begin by expanding the vehicle model and completing additional experimental validation. The model could be expanded by adding additional components which would further simulate real world conditions. To begin with, a tire-ground interaction model should be developed and added. This would allow for driving simulations which take into account slip and allows for testing of the skid steering of the vehicle. Following the tire model, a battery and motor model should be added. This would increase the value of the model for many reasons. In particular, this would allow for further simulation of the dozing optimization presented. The optimal blade angle could be input, a dozing job could be simulated, and the battery usage could be evaluated. With the addition of power consumption, the cost function metrics could be adjusted so that an acceptable amount of power and time is spent on a certain job. Finally, the simulation should be expanded to include back and forth travel and blade depth control so that it can simulate complete dozing jobs. This would allow for the user to test complete path planning algorithms which may eventually be used on the job site.

Following the significant expansion of the model discussed, further validation of the simulation should be completed. A blade should be attached to the robot and dozing tests should be run with different suspension configurations. This type of testing could validate the blade angle optimization presented as well as further validate the suspension optimization. Once this is completed, any further experiments which could validate the expansions to the model should also be completed. The model expansions and validations discussed would form a complete model of the robot which could be used for many design and application studies.

In addition to furthering the current model, this research has shown promise in the study of a variable angle blade design and an active suspension. The blade design shown here should be refined, constructed, and studied. In addition, the semi-active suspension system presented could be expanded to a fully active system. The effectiveness of this system could be evaluated in a simulation similar to the one presented here. If the simulation proved promising then a fully active system could be added to the robot and tested.

## References


[1] Bone, Garry M., et al. “Autonomous Robotic Dozing for Rapid Material Removal”. *Proceedings of the 30th ISARC, Montreal, Canada.* 2013

[2] Moore, P. “Return of the Robominers” *Mining Magazine, 195,16-22.* 2006

[3] Ito N. “Bulldozer Blade Control”. *Journal of Terramechanics, 28(1), 65-71.* 1991

[4] Onwualu, A.P. and K.C. Watts. “Draught and Vertical Forces Obtained From Dynamic Soil Cutting by Plane Tillage Tools”. *Soil & Tillage Research 48, 239-253,* 1998.

[5] McKyes, E. “Agricultural Engineering Soil Mechanics”. *Developments in Agricultural Engineering 10. Elsevier,* 1989.

[6] Singh, S. “Synthesis of Tactical Plans for Robotic Excavation”. *PhD Dissertation, Carnegie Mellon University. Pittsburgh, PA.* 1995

[7] Staford, J. V. “The Performance of a Rigid Tine in Relation to Soil Properties and Speed”.*The British society for Research in Agricultural Engineering. 24, 41-56,* 1979.

[8] Shaoqiang, Yuan, Liu Zhong, and Li Xingshan. "Modeling and simulation of robot based on Matlab/SimMechanics." *Control Conference, 2008. CCC 2008.27th Chinese*.IEEE, 2008.

[9] Wood, Giles D., and Dallas C. Kennedy."Simulating mechanical systems in Simulink with SimMechanics."*The Mathworks Report* , 2003.

[10] Yang, Chifu, et al. "Modeling and simulation of spatial 6-DOF parallel robots using Simulink and Simmechanics." *Computer Science and Information Technology (ICCSIT), 2010 3rd IEEE International Conference* on.Vol. 4.IEEE, 2010.

[11] Besselink, I. J. M. "Vehicle dynamics analysis usingSimMechanics and TNO Delft-Tyre." *IAC 2006 TheMathworks International Automotive Conference, Stuttgart, Germany*. 2006.